

1           **Mass-dependent Selenium Isotopic Fractionation during Microbial Reduction of**  
2                           **Seleno-oxyanions by Phylogenetically Diverse Bacteria**  
3

4   Kathrin Schilling<sup>1\*</sup>, Anirban Basu<sup>2</sup>, Christoph Wanner<sup>3</sup>, Robert A. Sanford<sup>4</sup>, Celine Pallud<sup>5</sup>,  
5                           Thomas M. Johnson<sup>4</sup>, Paul R.D. Mason<sup>6</sup>  
6

7   <sup>1</sup> *Lamont-Doherty Earth Observatory of Columbia University, Palisades, NY, USA*

8   <sup>2</sup> *Department of Earth Sciences, Royal Holloway, University of London, Egham, TW20 0EX,*  
9   *United Kingdom*

10 <sup>3</sup> *Institute of Geological Sciences, University of Bern, Baltzerstrasse 3, CH-3012 Bern,*  
11 *Switzerland*

12 <sup>4</sup> *Department of Geology, University of Illinois at Urbana-Champaign, Champaign, IL,*  
13 *61820, USA*

14 <sup>5</sup> *Department of Environmental Science, Policy and Management, University of California,*  
15 *Berkeley, 130 Mulford Hall, Berkeley, California, 94720, USA*

16 <sup>6</sup> *Department of Earth Sciences, Utrecht University, Princetonlaan 8A, 3584 CB Utrecht, The*  
17 *Netherlands*

18 \*Corresponding author: [kathrins@ldeo.columbia.edu](mailto:kathrins@ldeo.columbia.edu)

19 **Abstract**

20 Selenium (Se) isotope fractionation has been widely used for constraining redox conditions  
21 and microbial processes in both modern and ancient environments, but our knowledge of the  
22 controls on fractionation during microbial reduction of Se-oxyanions is based on a limited  
23 number of studies. Here we complement and expand the currently available pure culture data  
24 for Se isotope fractionation by investigating for the first time six phylogenetically and  
25 physiologically non-respiring bacterial strains that reduce Se-oxyanions to elemental Se  
26 [Se(0)]. Experiments were performed with either selenate [Se(VI)] or selenite [Se(IV)] at  
27 lower, more environmentally-relevant concentrations (9 to 47  $\mu\text{M}$ ) than previously  
28 investigated. *Enterobacter cloacae* SLD1a-1, *Desulfitobacterium chlororespirans* Co23 and  
29 *Desulfitobacterium sp.* Viet-1 were incubated with Se(VI) and Se(IV). *Geobacter*  
30 *sulfurreducens* PCA, *Anaeromyxobacter dehalogenans* FRC-W and *Shewanella sp.* (NR)  
31 were examined for their ability reducing Se(IV) to Se(0). Our data confirm that microbial  
32 reduction of both Se-oxyanions is accompanied by large kinetic isotopic fractionation  
33 (reported as  $^{82/76}\epsilon = 1000 * (^{82/76}\alpha - 1) \text{‰}$ ). Under our experimental conditions, microbial  
34 reduction of Se(VI) shows consistently greater isotope fractionation ( $\epsilon = -9.2\text{‰}$  to  $-11.8\text{‰}$ )  
35 than reduction of Se(IV) ( $\epsilon = -6.2$  to  $-7.8\text{‰}$ ) confirming the difference in metabolic pathways  
36 for the reduction of the two Se-oxyanions. For Se(VI), the inverse relationship between  
37 normalized cell specific reduction rate (cSRR) and Se isotope fractionation suggests that the  
38 kinetic isotope effect for Se(VI) reduction is governed by an enzymatically-specific pathway  
39 related to the bacterial strain-specific physiology. In contrast, the lack of correlation between  
40 normalized cSRR and isotope fractionation for Se(IV) reduction indicates a non-enzyme  
41 specific pathway which is dominantly extracellular. Our study highlights the importance to  
42 understand microbially-mediated Se isotope fractionation depending on Se species, and cell-  
43 specific reduction rates before Se isotope ratios can become a fully applicable tool to  
44 interpret Se isotopic changes in modern and ancient environments.

45

## 46 **1. Introduction**

47 Selenium (Se) isotope fractionation has been widely described in modern environments as  
48 well as in ancient settings preserved in sedimentary rocks (Herbel et al., 2002; Mitchell et al.,  
49 2012; Wen and Carignan, 2011; Wen et al., 2014; Schilling et al., 2015; Stüeken et al.,  
50 2015a, b; Basu et al., 2016; Kipp et al., 2017). Selenium stable isotopes are particularly  
51 sensitive to redox reactions, which determine chemical Se speciation in the environment. The  
52 most mobile and bioavailable forms of Se are the water-soluble oxyanions selenate [Se(VI)]  
53 and (hydro)selenite [Se(IV)]. Selenate is the dominant redox state in modern surface waters  
54 (Martin et al., 2011) while Se(IV) is present in ocean surface water, but adsorbs strongly onto  
55 iron, manganese and aluminum oxides (Parida et al., 1997; Peak and Sparks, 2002; Peak,  
56 2006) as well as clays. Sparingly soluble elemental Se [Se(0)] and selenide [Se(-II)] are the  
57 dominant redox states in anoxic environments. Typically, environmental Se concentrations  
58 are at sub-micromolar levels (Conde and San Alaejos, 1997; Fordyce, 2013) but can locally  
59 be elevated in sulfide ores and roll-front type uranium ores (Howard, 1977; Basu et al.,  
60 2016), shales (Pogge von Strandmann et al., 2015; Stüeken et al., 2015a) or by anthropogenic  
61 pollution. (*e.g.*, Presser and Ohlendorf, 1987; Dreher and Finkelman, 1992; Lemly, 2004;  
62 Muscatello et al., 2008). Because the mobility and environmental impact of Se are  
63 determined by its chemical speciation, it is important to understand the environmental  
64 processes that control Se speciation and transitions between oxidation states.

65 Microbial reduction of Se-oxyanions is the primary set of reactions generating solid Se(0) in  
66 natural settings. Both Se-oxyanions are energetically favourable electron acceptors because  
67 the reduction of Se(IV) or Se(VI) can provide 90 to 150 times more free energy ' $\Delta G$ ' (- 8.9 to -  
68 15.5 kcal mol<sup>-1</sup>e<sup>-1</sup>) for bacteria than the reduction of sulfate to sulfide (Stolz and Oremland,  
69 1999). Bacteria able to reduce Se-oxyanions are phylogenetically diverse, have different  
70 metabolic strategies, and have been isolated from both oxic and anoxic environments (*e.g.*,

71 Macy et al., 1993; Herbel et al., 2000; Stolz et al., 2006; Yee and Kobayashi, 2008; Pearce et  
72 al., 2009). All microorganisms are facultative and it has been shown that non-specific  
73 metabolic Se reduction can involve different enzyme systems, e.g. for reduction of nitrite,  
74 nitrate, arsenate, sulfate and glutathione (*e.g.*, Switzer Blum et al., 1998; Sabaty et al., 2001;  
75 Kessi and Hanselmann, 2004; Basaglia et al., 2007). Few Se(VI)-reducing bacteria have been  
76 identified to catalyze Se(VI) reduction by the Se-specific enzyme selenate reductase  
77 (Schröder et al. 1997; Bébien et al., 2002; Ridley et al., 2006, Theissen and Yee, 2014) and  
78 only two bacterial strains (*Tetrathioibacter kashmirensis* and *Pseudomonas sp.*) have a  
79 Se(IV)-specific enzyme (Hunter and Manter, 2008, 2009).

80 Limited published data on Se isotope fractionation during microbial Se reduction have  
81 revealed large variations (Herbel et al., 2000; Ellis et al., 2003, Clark and Johnson, 2008). A  
82 previous study with pure cultures (*Bacillus selenitireducens*, *Bacillus arsenicoselenatis* and  
83 *Sulfurospirillum barnesii*) was restricted to dissimilatory Se-reducing bacteria grown with  
84 very high millimolar levels of Se (10 – 20 mM) and with only lactate as electron donor at  
85 high concentrations (10 – 40 mM). For these conditions, the reported Se isotope fractionation  
86 varied greatly between -1.7 and -13.7‰ for the reduction of Se(IV) to Se(0) and -1.7 and -7.5  
87 ‰ for reduction of Se(VI) to Se (IV) (Herbel et al., 2000). At contaminated sites, however,  
88 Se concentrations are two to three orders of magnitude lower with Se concentration up to 150  
89 µM (= 12,000 µg/L) in agricultural drainage and irrigation water (Deverel and Fujii, 1988;  
90 Meseck and Cutter, 2011; Schilling et al., 2015) and up to 12 µM (= 955 µg/L) in waste  
91 water from Se-bearing phosphorite mining (Mars and Crowley 2003; Stiling and Amacher,  
92 2010). Even lower Se concentrations occur in modern ocean and aquifers with average values  
93 of 0.002 µM and 0.5 µM Se, respectively (*e.g.*, Conde and San Alaejos, 1997; Pearce et al.,  
94 2009; Basu et al., 2016).

95 Another study using sediments slurries reported Se isotopic fractionation by resident Se-  
96 reducing microbial community between -8.3 and -8.6‰ for the reduction of Se(IV) to Se(0)  
97 and -3.9 and -4.7‰ for the reduction of Se(VI) to Se(IV) (Ellis et al., 2003). Resident Se-  
98 reducing microbial communities comprise diverse groups of bacteria with different metabolic  
99 strategies. Although the magnitude of Se isotope fractionation by microbial reduction of Se-  
100 oxyanions has been previously studied, the cause of such large variation in  $\epsilon$  values and their  
101 relevance for environmental settings remains unclear.

102 In this study, we extend the currently available experimental data by determining the isotopic  
103 fractionation during microbial reduction of Se-oxyanions [Se(VI), Se(IV)] that includes  
104 previously unexplored groups of mesophilic bacteria (Fig. 1), with the first results for  
105 bacteria that perform non-catabolic reduction of Se-oxyanions. To investigate whether  
106 different Se metabolic strategies affect the magnitude of isotopic fractionation, we selected  
107 bacterial strains based on their ubiquitous distribution and their well-studied metabolisms.  
108 For Se(VI) reduction, we conducted experiments with the Gram-negative bacterium  
109 *Enterobacter cloacae* SLD1a-1, and the Gram-positive bacteria *Desulfitobacterium* sp. Viet-  
110 1, and *Desulfitobacterium chlororespirans* Co23. For the reduction of Se(IV), we used  
111 isolates of three Gram-negative bacteria namely *Geobacter sulfurreducens* PCA,  
112 *Anaeromyxobacter dehalogenans* FRC-W and *Shewanella* sp. (NR) in addition to the three  
113 Se(VI)-reducing bacterial strains. Studying pure bacterial cultures has the advantage to  
114 eliminate any complexity from natural microbial communities such as competing strains with  
115 possibly different reduction rates and to determine isotopic fractionation linked to a single  
116 reduction mechanism. Further, we used lower electron acceptor and electron donor  
117 concentrations compared to previous studies to achieve slow Se reduction rates as it is well  
118 established that rapid reductions are transport limited and suppress the overall isotopic  
119 fractionation (Clark and Johnson, 2010). These experimental conditions are very close to Se

120 concentrations reported for Se contaminated groundwater, soils, porewater (*i.e.*, Meseck and  
121 Cutter, 2011; Stiling and Amacher, 2010; Schilling et al., 2015; Basu et al., 2016).

## 122 **2. Materials and Methods**

### 123 *2.1 Microbial culture*

124 The strains, *Desulfitobacterium sp.* Viet-1, *Desulfitobacterium chlororespirans* Co23,  
125 *Geobacter sulfurreducens* PCA, *Aneromyxobacter dehalogenans* FRC-W and *Shewanella sp.*  
126 (NR) (Table 1) were supplied by Sanford, and *Enterobacter cloacae* SLD1a-1 (Table 1) was  
127 supplied by Pallud. For initial growth of bacterial cultures and for Se reduction experiments,  
128 we used the mineral-salt medium described by He and Sanford (2002). One liter of test  
129 medium was prepared with 10 mL buffer (12.5 g KH<sub>2</sub>PO<sub>4</sub>, 20.0 g K<sub>2</sub>HPO<sub>4</sub> per liter), 10 mL  
130 trace salt (1.17 g CaCl<sub>2</sub>, 2.00 g MgCl<sub>2</sub> × 6H<sub>2</sub>O, 0.70 g FeSO<sub>4</sub> × 7H<sub>2</sub>O, 0.50 g Na<sub>2</sub>SO<sub>4</sub> per  
131 liter), 1 mL trace metals (0.05 g ZnCl<sub>2</sub>, 0.5 g MnCl<sub>2</sub> × 4H<sub>2</sub>O, 0.03 g CuCl<sub>2</sub> × 2H<sub>2</sub>O, 0.05 g  
132 CoCl<sub>2</sub> × 6H<sub>2</sub>O, 0.05 g H<sub>3</sub>BO<sub>3</sub>, 0.05 g NiSO<sub>4</sub> × 6H<sub>2</sub>O, 0.01 g Na<sub>2</sub>MoO<sub>4</sub> × 2H<sub>2</sub>O, 0.004 g  
133 Na<sub>2</sub>WO<sub>4</sub>), 1 mL ammonium chloride, 1 mL selenium-tungsten and 0.84 g NaHCO<sub>3</sub>. The  
134 growth medium was supplemented with 0.03 g L-cysteine while the reductant L-cysteine was  
135 omitted for the test medium used for Se batch experiments. Anaerobic condition in both  
136 growth and test media was generated by boiling and degassing with N<sub>2</sub>/CO<sub>2</sub> mix, the  
137 subsequent transfer into 120 mL glass serum bottles sealed with butyl rubber stoppers, and  
138 autoclaving at 121°C for 30 min.

139 In the growth medium, the bacterial strains *Desulfitobacterium chlororespirans* Co23 and  
140 *Desulfitobacterium sp.* Viet-1 were initially grown under fermentative conditions using 10  
141 mM pyruvate and *Enterobacter cloacae* SLD1a-1 using 2 mM glucose. *Shewanella sp.* (NR)  
142 was incubated with 1 mM nitrate and 2.5 mM lactate. *Anaeromyxobacter dehalogenans* FRC-  
143 W was incubated with 2.5 mM acetate and 1.25 mM nitrate. *Geobacter sulfurreducens* PCA  
144 was grown with 3 mM acetate as electron donor and 10 mM fumarate as electron acceptor.

145 All anaerobic cultures were incubated at 30°C for 3 to 5 days to achieve high cell densities  
146 ( $\sim 10^{10}$  cells mL<sup>-1</sup>) and complete consumption of the growth substrates.

## 147 2.2 Seleno-oxyanions reduction experiments

148 To test the reduction of Se-oxyanions, 10 mL of inoculum from the growth cultures,  
149 corresponding to bacterial densities of  $10^5$  - $10^7$  cells mL<sup>-1</sup> (Table 2) were transferred to the  
150 test medium. The microbial cultures were amended with 10 to 47  $\mu$ M Se(VI) or Se(IV) as the  
151 sole terminal electron acceptor. Depending on the bacterial strain, 500  $\mu$ M (2,000 and 10,000  
152  $\mu$ M for *Geobacter sulfurreducens* PCA) acetate or lactate as electron donor was added to  
153 each reactor (Table 1, 2). The experiments containing Se-oxyanions were conducted without  
154 any chemical reducing agent to minimize any cell reproducibility and to avoid any abiotically  
155 mediated Se reduction. The “no-cell” control experiments were carried out using identical  
156 concentrations of electron donor and Se(VI) or Se(IV), but without any cell suspension. To  
157 identify if viable cells were responsible for Se reduction, a “heat-killed cell” control of  
158 *Desulfitobacterium chlororespirans* Co23 (autoclaved for 30 minutes) was inoculated with  
159 18  $\mu$ M Se(VI) and 500  $\mu$ M lactate as electron donor. All cultures were incubated  
160 anaerobically at 30°C under continuous shaking, and sampled at regular time intervals for  
161 periods ranging from 60 to 800 hours, depending on the bacterial strains. Subsamples were  
162 filtered through 0.2  $\mu$ m nylon filters.

## 163 2.3 Determination of cell-specific reduction rate (cSRR)

164 A 1 mL aliquot of each culture was sampled for cell counting at the beginning of the  
165 experiment (t = 0). Cells were prefixed in 8% formaldehyde and stored at 4°C until analyzed.  
166 Bacterial cells were stained with 1  $\mu$ L of the STYO bacterial stain and 10  $\mu$ L of microsphere  
167 standard (bacteria counting kit, Invitrogen). The cell counting was performed by flow  
168 cytometry analysis using a LSR II analyzer (BD Biosciences). The cell density was

169 determined from the cell-counts for a known number of microspheres in each sample. Culture  
170 cell density values were used to calculate the initial cell density in the batch experiments and  
171 to calculate the cell specific Se reduction rate (cSRR) using the following expression:

$$172 \quad \text{cSRR} = \Delta c / t_{1/2} \times d_0 \quad (\text{Eq. 1})$$

173 where  $\Delta c$  is the decrease in Se(VI) or Se(IV) concentration at the half-life  $t_{1/2}$ , and the initial  
174 cell density  $d_0$ . All cSRR values were normalized relative to the initial Se concentrations.

#### 175 *2.4 Transmission electron microscopy (TEM)*

176 Microbial cultures of *Enterobacter cloacae* SLD1a-1 were incubated with Se(VI) or Se(IV)  
177 for 24 hours. Afterwards the bacterial cells were pre-concentrated by centrifugation and fixed  
178 with 2% glutaraldehyde in a 0.04 M phosphate buffer. After the second cell fixation using 1%  
179 osmium tetroxide, the samples were dehydrated with different concentrated ethanol  
180 solutions and embedded in resin. After sectioning of the bacterial cells, micrographs were  
181 taken with a Technai 12 transmission electron microscope (University of California,  
182 Berkeley).

#### 183 *2.5 Se isotope and concentration analysis*

184 Initially, the concentrations of dissolved Se species [Se(VI) and/or Se(IV)] were measured  
185 using mass  $^{78}\text{Se}$  by hydride generation-inductively coupled plasma-mass spectrometry (ICP-  
186 MS). Prior to measurement, Se(VI) was converted to Se(IV) by heating at 105°C degrees for  
187 60 minutes in a 5 M HCl matrix. The reported Se concentrations were calculated using an  
188 isotope dilution double-spike method by adding  $^{74}\text{Se} + ^{77}\text{Se}$  double spike of known isotope  
189 ratio and concentration to the sample with unknown Se concentration (*e.g.*, Heumann, 1992).  
190 We also used double spike isotope technique with an approximate sample spike proportion of  
191 2 to correct for isotopic fractionation during sample purification and instrumental mass bias  
192 during the isotope measurement.



193 Selenium species separation from matrix solutes was performed using 1 mL AG1-X8 anion-  
194 exchange resin (Eichrom). Prior to anion-exchange, all subsamples of Se(IV) were oxidized  
195 to Se(VI) with a 20 mM solution of the strong oxidizer potassium persulfate (Schilling et al.,  
196 2014, 2015) prior to heating at 90°C for 1h. The sample purification procedure (including an  
197 oxidation step for Se(IV) and chromatographic separation for all samples) resulted in  
198 recoveries of >90%.

199 Selenium isotope ratios were measured using a Nu Plasma high resolution multiple collector-  
200 ICP-MS, connected to a custom-built hydride generation system described in previous studies  
201 (e.g., Clark and Johnson, 2008; Mitchell et al. 2012; Zhu et al., 2014; Schilling et al., 2015;  
202 Mitchell et al., 2016). All  $^{82}\text{Se}/^{76}\text{Se}$  ratios are reported as  $\delta$  notation relative to the NIST SRM  
203 3149 inter-laboratory standard:

$$204 \quad \delta = \frac{R_{\text{sample}}}{R_{\text{standard}}} - 1 \quad (\text{Eq. 2})$$

205 Blank solutions processed through the same sample purification procedure contained an  
206 average of  $4.4 \pm 2.9$  ng Se (n=12), less than 0.7% of the total sample. The uncertainty on  
207  $\delta^{82/76}\text{Se}$  was estimated by calculating the root mean square difference (RMS) for samples  
208 prepared and analyzed in duplicate (n = 25). The in-house standard MH-495 was measured  
209 with an average value of  $-3.35 \pm 0.1\%$  ( $2\sigma$ , n = 12) relative to SRM-3149 within excellent  
210 agreement of previously reported values (Carignan and Wen, 2007; Zhu et al., 2008).  
211 Average external  $^{82/76}\text{Se}$  precision was  $\pm 0.16\%$  based on repeated analysis of SRM-3149  
212 standards (n = 145) over two years. The external reproducibility for  $^{82/76}\text{Se}$  of the samples,  
213 determined as twice root mean square, was  $\pm 0.17\%$  (n = 25) across a range of  $\delta^{82/76}\text{Se}$  values  
214 between -0.3‰ and +29.3‰.

215 *2.6 Determination of the magnitude of isotopic fractionation ( $\epsilon$ )*

216 As all experiments were conducted in sealed batch reactors, the experiments were assumed to  
217 follow closed system behavior. Positive  $\delta^{82/76}\text{Se}$  values of the remaining, unreacted Se thus  
218 indicate enrichment in heavy isotopes relative to the standard, whilst negative values  
219 represent depletion of heavy isotopes. Changes in  $\delta^{82/76}\text{Se}$  can be directly related to the extent  
220 of Se(VI) or Se(IV) reduction. The magnitude of Se isotope fractionation was determined for  
221 each experiment by fitting the measured  $\delta^{82/76}\text{Se}$  values to Rayleigh distillation models  
222 following the method described by Scott et al. (2004):

223 
$$\delta^{82/76}\text{Se} = \left( \frac{c(t)}{c_0} \right)^{\alpha} - 1 \quad \text{---} \quad \text{(Eq.3)}$$

224 where  $c(t)$  and  $\delta(t)$  are the concentration and the isotopic composition of the remaining  
225 reactant (Se(VI) or Se(IV)) in solution as a function of reaction time. The fractionation factor  
226 ( $\alpha$ ) is defined as defined as  $\alpha = R_{\text{product}}/R_{\text{reactant}}$ , where R is the measured  $^{82}\text{Se}/^{76}\text{Se}$ , and often  
227 expressed in terms of  $\varepsilon$  (a per mil quantity) as

228 
$$\varepsilon = \left( \alpha - 1 \right) \times 1000 \quad \text{(Eq. 4)}$$

229 The magnitude of isotopic fractionation,  $\varepsilon$ , was calculated from the corresponding slope from  
230 the linear regression of  $\ln(\delta^{82}\text{Se} + 1000)$  versus  $\ln(c(t)/c_0)$ .

### 231 2.7 Statistical analysis

232 One-way analysis of variance (ANOVA) with Tukey-HSD test ( $\alpha = 0.05$ ) was used to  
233 evaluate the potential difference in the magnitude of Se isotope fractionation ( $\varepsilon$ ) between  
234 Se(IV) or Se(VI) reduction by the different bacterial strains and among the different bacterial  
235 strains. The statistical analyses were performed using JMP software 13.1.0. with a statistical  
236 probability of  $P < 0.05$ .

## 237 3. Results

### 238 3.1 Microbial reduction of Se(VI)

239 Figure 2 shows Se(VI) removal over time during anaerobic microbial Se(VI)-reduction  
240 experiments by three bacterial strains (*Enterobacter cloacae* SLD1a-1, *Desulfitobacterium*  
241 *chlororespirans* Co23, *Desulfitobacterium sp.* Viet-1). In the presence of Se(VI)-reducing  
242 bacteria, the decrease in Se(VI) concentration ranged between 51% to 99% relative to the  
243 initial Se(VI) concentrations in the batch reactors. In all experiments, the decrease in Se(VI)  
244 concentration with time follows a first-order kinetics except for the latest sampling points. A  
245 single first-order rate constant reasonably fit all data from each experiment. The heat-killed  
246 control with bacterial cells from *Desulfitobacterium chlororespirans* Co23 did not show any  
247 measurable Se(VI) removal after ca. 4 days of incubation (Figure 2A). We observed in the  
248 batch reactors an initial increase in Se(IV) resulting from the reduction of Se(VI), followed  
249 by Se(IV) reduction to Se(0) (Table A1).

250 In all Se(VI) experiments, an enrichment of  $^{82}\text{Se}$  occurred in the remaining unreacted Se(VI)  
251 with progressive Se(VI) reduction (Figure 3). The largest  $\delta^{82/76}\text{Se}$  value of +38.6‰ was  
252 observed at 99% reduction of Se(VI) for the experiment with *Desulfitobacterium sp.* Viet-1  
253 (Figure 3C). The  $\delta^{82/76}\text{Se}$  values for the intermediate Se(IV) varied between -9.6‰ for 1.5%  
254 Se(IV) and 16.6‰ for 15% Se(IV) relative to the initial Se(VI) concentration (9  $\mu\text{M}$ ) (Table  
255 A1). The magnitudes of Se isotopic fractionation ( $\epsilon$ ) for microbial Se(VI) reduction, obtained  
256 by fitting  $\delta^{82/76}\text{Se}$  data to Eq. 3, are illustrated in Figure 3 and reported in Table 3. Among the  
257 three Se(VI)-reducing pure bacterial cultures, the  $\epsilon$  values varied between -9.2‰ and -11.8‰  
258 with a mean value of  $-10.6 \pm 1.3\text{‰}$ . The  $\epsilon$  values did not deviate in duplicate reactors within  
259 a  $2\sigma$  uncertainty limit. The initial cell densities varied by two orders of magnitude in the  
260 Se(VI) incubation with the highest cell density of  $1.9 \times 10^8 \text{ cell ml}^{-1}$  for the batch of  
261 *Enterobacter cloacae* SLD1-1a. The normalized cSRR ranged from  $0.11 \times 10^{-17}$  to  $1.30 \times 10^{-17}$   
262  $\text{mol Se(VI) cell}^{-1} \text{ d}^{-1}$  (Table 2). We observed a strong inverse relationship ( $r^2 = 0.91$ ) between

263 normalized cSRR and  $\epsilon$  for Se(VI) reduction with decreasing  $\epsilon$  values for increasing values of  
264 cSRR (Figure 4A).

265 Transmission electron microscope images of a washed cell suspension of *Enterobacter*  
266 *cloacae* SLD1a-1 after the reduction of Se(VI) showed intracellular Se(0) precipitates (Figure  
267 5A). The particle sizes were spherical,  $<0.2 \mu\text{m}$  in diameter and located in the periplasmic  
268 space.

### 269 3.2. Microbial reduction of Se(IV)

270 Anoxic batch incubations of six Se-reducing bacterial strains with Se(IV) showed a decrease  
271 in Se(IV) concentration as a function of time (Figure 6 and Table A2). The Se(IV) removal  
272 ranged between 56% to 92% over a period of 0.4 to 6.1 days. The no-cell control experiments  
273 did not show any change in Se(IV) concentrations with time. In each experiment, a first order  
274 kinetic model with a single rate constant fits all Se(IV) concentration data. The time interval  
275 for 50% removal of the initial Se(IV) concentration varied from 0.42 to 3.1 days. *Geobacter*  
276 *sulfurreducens* PCA assayed with varying electron donor concentrations (2,000 to 10,000  
277  $\mu\text{M}$ ) exhibited an approximately 50% Se(IV) removal after similar time periods ( $t_{1/2}$  0.49 to  
278 0.66 days).

279 The initial cell densities varied by approximately two-orders of magnitudes depending on the  
280 volume of inoculum. The highest cell density was found for the Se(IV) batch of  
281 *Anaeromyxobacter dehalogenans* FRC-W ( $1.3 \times 10^8 \text{ cell ml}^{-1}$ ) and the lowest for  
282 *Enterobacter cloacae* SLD1a-1 ( $8.8 \times 10^6 \text{ cell ml}^{-1}$ ). The calculated cell-specific reduction rate  
283 ranged from 0.28 to  $5.7 \times 10^{-17} \text{ mol cell}^{-1} \text{ d}^{-1}$  with no correlation between normalized cSRR  
284 and  $\epsilon$  values ( $r^2 = 0.13$ ; Figure 3B). We observed no correlation between normalized cSRR  
285 and  $\epsilon$  for Se(IV) reduction (Figure 4B).

286 While the Se(IV) concentration in the batch reactors decreased,  $\delta^{82/76}\text{Se}$  progressively  
287 increased with time (Figure 7) relative to the starting Se(IV). The duplicate batch reactors

288 showed similar  $\epsilon$  values within the  $2\sigma$  uncertainty level of  $\pm 0.12\text{‰}$  to  $\pm 0.43\text{‰}$ . (Table 3). The  
289 largest  $\delta^{82/76}\text{Se}$  value of  $+15.7\text{‰}$  was observed for *Shewanella sp.* (NR) after 91% Se(IV)  
290 removal. The  $\epsilon$  values for Se(IV) reduction span a narrow range of  $-6.2\text{‰}$  to  $-7.8\text{‰}$  with a  
291 mean value of  $-7.0 \pm 0.6\text{‰}$ . We observed no significant difference in  $\epsilon$  values among the six  
292 different bacterial strains ( $p = 0.376$ ; Figure 7).

293 Transmission electron microscope images of *Enterobacter cloacae* SLD1a-1 incubated with  
294 Se(IV) showed exogenous precipitates, presumably Se(0) (Figure 5A) which are smaller than  
295 the intracellular Se(0) particles observed as a product of Se(VI) reduction (Figure 5B).

## 296 **4. Discussion**

297 Our results demonstrate that the magnitude of Se isotope fractionation by microbial reduction  
298 of Se-oxyanions depends mainly on two factors (1) growth conditions and (2) the Se-  
299 reduction by cometabolic or Se-respiring pathway. Below we discuss variation in Se isotope  
300 fractionation based on these two factors, specifically in the context of previous studies.  
301 Differences in the magnitude of Se isotope fractionation in our study compared to the  
302 previous studies (Herbel et al., 2000; Ellis et al., 2003; Clark and Johnson, 2008) is attributed  
303 to differences in the experimental approach and selection of bacterial strains.

### 304 *4.1. Effect of experimental conditions on $\epsilon$*

305 In the following section we discuss the reasons behind differences in the magnitude of Se  
306 isotope fractionation between our study and previous studies (Herbel et al., 2000; Ellis et al.,  
307 2003; Clark and Johnson, 2008).

#### 308 *4.1.1 Comparison to pure culture studies*

309 Environmentally-relevant conditions, more specifically much lower Se substrate  
310 concentrations, result in a narrower-range Se isotope fractionation factors for the reduction of  
311 both Se(VI) and Se(IV) compared to previously published values obtained for *Bacillus*

312 *selenitireducens*, *Bacillus arsenicoselenatis* and *Sulfurospirillum barnesii* (Herbel et al.  
313 2000). Indeed, Herbel et al. (2000) experiments were conducted under highly optimum  
314 growth conditions for anaerobic Se respiration *i.e.*, using high initial Se-oxyanion  
315 concentrations (10 - 20 mM) and high carbon concentrations (10 - 40 mM). This led to fast  
316 reduction rates and 100-fold increase in cell density during the experiment, which might  
317 explain the large span in isotopic fractionation they observed for Se(VI) reduction ( $\epsilon = -1.7$  to  
318  $-7.5\%$ ; Herbel et al., 2000). In addition, Se reduction rates in the previous study were one-  
319 order of magnitude ( $10^{-16}$  mol cell<sup>-1</sup> d<sup>-1</sup>) higher than the cSRRs observed in our experiments  
320 ( $10^{-17}$  mol cell<sup>-1</sup> d<sup>-1</sup>). In contrast to the large increase in cell density in the experiment by  
321 Herbel et al (2000), natural microbial consortia generally maintain a rather steady state  
322 population where cell decay balances cell growth (Brock, 1971). The more uniform  $\epsilon$  values  
323 in our study correspond to minor cell growth or decay evident from single first-order rate  
324 constants fitting the time series from each experiment and thus more consistent cSRRs  
325 throughout the experiment. Moreover, three-orders of magnitude lower initial Se-oxyanions  
326 concentrations, together with 20 times lower carbon concentrations as electron donor (10 mM  
327 vs. 0.5 mM), led to significantly larger  $\epsilon$  values ( $\epsilon = -9.2\%$  to  $-11.8\%$ ). Likewise, our data on  
328 microbial Se(IV) reduction result in an overall narrow distribution of  $\epsilon$  values ( $\epsilon_{\text{mean}} = -7 \pm$   
329  $0.6\%$ ) compared to the previous study ( $\epsilon = -1.7$  to  $-13.7\%$ ; Herbel et al., 2000). This narrow  
330 range of  $\epsilon$  values is likely when the tested strains are not actively respiring Se. Instead, the  
331 reduction of Se-oxyanions is a response to cope with the element's toxicity. Lower initial  
332 Se(IV) concentration also affect the results in two different ways by producing lower  
333 reduction rates and lower Se concentrations are less toxic for the cells and thus maintains the  
334 cell viability.

335 Whether bacteria reduce Se as respiration pathway (Herbel et al., 2000) or as a cometabolic  
336 pathway determines the magnitude of isotope fractionation. All bacterial strains (*Bacillus*

337 *selenitireducens*, *Bacillus arsenicoselenatis* and *Sulfurospirillum barnesii*) used in Herbel et  
338 al. (2000) are capable of actively metabolizing Se oxyanions. This means that the bacteria are  
339 able to harness the energy derived from coupling reduction of Se(VI)/Se(IV) and oxidation of  
340 lactate to synthesize biomass. This leads to bacterial growth (increase of cell density by about  
341 two orders of magnitude) during the experiments which changes the cSRR and thus affects  
342 the  $\epsilon$  values. For example, isotope fractionation by *Bacillus selenitireducens* varied between -  
343 2.6 and -13.7‰ (Herbel et al., 2000). This also explains why the relationship between cSRR  
344 vs.  $\epsilon$  breaks down for Se-respiring bacteria. Further, both Se(VI)-respiring bacterial strains,  
345 *Bacillus arsenicoselenatis* and *Sulfurospirillum barnesii*, only reduce a very small amount of  
346 Se(IV) to Se(0) (Herbel et al., 2000), while our tested bacterial strains reduce Se(VI) all to  
347 Se(0) (Table A1).

348 Although the tested Se-reducers are not confined to any particular group of bacteria (Figure  
349 1), we demonstrate that not the phylogenetic differences but the metabolic mechanisms  
350 control Se isotope fractionation. There is no systematic difference in  $\epsilon$  between the tested  
351 non-respiring Gram-positive (*Desulfitobacteria*) and Gram-negative bacteria (*Enterobacter*  
352 *cloacae* SLD1a-1). Gram-negative bacteria possess two membranes separated by the  
353 periplasmic space. The selenate reductase of Gram-negative bacterium *Enterobacter cloacae*  
354 SLD1a-1 is a membrane-bound enzyme situated in the cytoplasmic (inner) membrane  
355 (Schröder et al., 1997; Bébien et al., 2002; Ma et al., 2009). The location for the Se(VI)-  
356 reducing enzymes of *Desulfitobacterium chlororespirans* Co23 and *Desulfitobacterium sp.*  
357 Viet-1 are not known but are probably also membrane-bound as described for other Se(VI)-  
358 reducing Gram positive bacteria (Kuroda et al., 2011). Hence, the diffusive transport across  
359 the outer membrane for Gram-negative bacteria seems not to affect the reaction rate and Se  
360 isotope fractionation for Se(VI) reduction.

361 In bacterial strains with no Se-specific enzymatic pathway, the reduction is carried out by  
362 various enzyme systems, e.g. nitrite reductase, nitrate reductase, arsenate and sulfate  
363 reductases, or the reduction of Se(IV) by glutathione (*e.g.*, Tomei et al., 1995; Switzer Blum  
364 et al., 1998; Sabaty et al., 2001; Kessi and Hanselmann, 2004; Basaglia et al., 2007;  
365 Nancharaiah and Lens, 2015). These enzyme systems have mainly a detoxifying function and  
366 the energy released by the redox reaction is not generally utilized to synthesize biomass.  
367 Therefore, we assume that the obtained isotope fractionation factors can be extrapolated to a  
368 much wider group of microorganisms because the studied pure cultures include bacteria with  
369 different cell membranes (Gram positive and Gram negative), different enzymes in the  
370 electron transfer chain (*e.g.*, selenate reductase for *Enterobacter cloacae*) and carbon  
371 substrates (acetate and lactate) but show nearly identical isotope fractionations for the  
372 reduction of the respective Se-oxyanion.

#### 373 4.1.2 Comparison to natural microbial consortia in sediment slurries and cores

374 Our pure culture microbial Se(VI) reduction experiments induced significantly larger Se  
375 isotope fractionation than experiments with sediment slurries and sediment cores involving  
376 complex microbial communities (Ellis et al., 2003; Clark and Johnson, 2008). Here reported  $\epsilon$   
377 values relate to suspensions of free-living cells with maximized mass transfer and  
378 accessibility of Se-oxyanions for each bacterial cell. Mass transfer limitation in sediment  
379 slurries and cores is expected to decrease the exchange between Se(VI) in solution and the  
380 particle-bound bacteria. This in turn should reduce selectivity for an isotopologue (heavy vs.  
381 light). Generally, mass transfer is faster for the isotopically light  $^{76}\text{Se}$ -oxyanions than for the  
382 isotopically heavy  $^{82}\text{Se}$ -oxyanions. If the probability for Se(VI) selectivity of an isotopologue  
383 is limited for the particle-bound bacteria the mass transfer affects the Se isotope fractionation.  
384 This presumably explains the relatively small Se isotope fractionation observed in sediment  
385 slurries (Ellis et al., 2003) where the contact between bacteria and Se-oxyanions in solution is



386 limited but still higher than for sediment cores (Clark and Johnson, 2008). Selenium isotope  
387 signals in sediments controlled by the diffusion of Se from the overlying water have the  
388 highest mass transfer limitation determined by incomplete solution exchange at the water-  
389 sediment interface and the lowest Se isotope fractionation of 0.4‰ for microbial Se  
390 reduction. In contrast, pure cultures in our study are more selective to a particular Se  
391 isotopologue (heavy vs. light) as they are not particle-bound. However even if in porewaters,  
392 diffusion limitation yields a smaller Se isotope fractionation the reduction of Se(VI) and  
393 Se(IV) are still detectable because the shift in  $\delta$  values from the initial value is significant.

#### 394 4.2. Effect of metabolic pathway on Se isotope fractionation

395 Reduction of Se-oxyanions occurs intracellularly in the periplasmic space for Se(VI) (*i.e.*,  
396 Ridley et al., 2006; Nancharaiah and Lens, 2015) or extracellularly for Se(IV) (*e.g.*, Pearce et  
397 al., 2009; Nancharaiah and Lens, 2015). Our data and the pure culture study by Herbel et al.,  
398 (2000) confirm that the pathways for reduction of Se(VI) or Se(IV) determine the Se isotope  
399 fractionation. Microbial Se(VI) reduction induces significantly larger fractionation than  
400 Se(IV) reduction for the six tested bacterial strains ( $p > 0.01$ ).

##### 401 4.2.1 Intracellular Se(VI) reduction

402 The reduction Se(VI) to Se(0) is a sequential two-step reaction which leads to significantly  
403 larger fractionation than Se(IV) reduction for the tested bacterial strains ( $p > 0.01$ ). The  
404 reduction of Se(VI) to Se(IV) *via* two electron transfer is followed by a four electron transfer  
405 to form Se(0). Heat-killed control experiments with *Desulfitobacterium chlororespirans*  
406 Co23, which did not show Se(VI) reduction and any concomitant Se isotopic fractionation,  
407 confirms that Se(VI) reduction is enzymatically-mediated by viable cells. Correlation  
408 between normalized cSRR and  $\epsilon$  for Se(VI) reduction indicates that the rate of electron  
409 transfer depends on the abundance of bacteria and their enzymes (*e.g.*, selenate reductase)

410 (Yee and Kobayashi, 2008). Mechanistically, diffusion transport brings Se(VI) to the  
411 reduction site of the bacterial cell where Se(VI) is then reduced intracellularly. As diffusive  
412 transport of Se(VI) does not involve changes in coordination of oxygen around Se, any  
413 discrimination between the isotopologes in the Se-oxyanions will be minor compared to  
414 enzymatic reduction. If the reduction rate of Se(VI) at these reduction sites is very slow either  
415 due low abundances of bacteria and their enzymes it is expected that  $\epsilon$  reaches a maximum  
416 value. Future studies can help determining the maximum value as well as the more in-depth  
417 understanding of the relevant enzymes involved in the cometabolic Se(VI) reduction and the  
418 related Se isotope fractionation.

#### 419 4.2.2 Extracellular Se(IV) reduction.

420 The four electron transfer by only one reduction step for Se(IV) explains the smaller Se  
421 isotope fractionation compared to the reduction of Se(VI). Electron transfer for the reduction  
422 of Se(IV) is driven by either an exogenous electron shuttle, extracellular proteins or possibly  
423 pili structures (Pearce et al., 2009). This also explains why the magnitude of Se isotope  
424 fractionation does not correlate with normalized cSRRs (Figure 4C) because an exogenous  
425 electron transfer does not require a direct contact between the bacterial cell and the substrate  
426 via a specific enzyme. Such extracellular reaction is also most likely decoupled from electron  
427 donor oxidation, so that different donor types or concentrations do not affect the isotope  
428 fractionation factor. This is clearly shown for the experiments with *Geobacter sulfurreducens*  
429 PCA, known for reducing Se(IV) extracellularly by outer membrane cytochromes (Pearce et  
430 al., 2009). Varying concentrations of electron donor (500 to 10,000  $\mu\text{M}$ ) have no effect on  $\epsilon$   
431 values (Table 3) for Se(IV) reduction by *Geobacter sulfurreducens* PCA. This is consistent  
432 with the observation for microbial Cr(VI) reduction where an extracellular Cr reduction  
433 pathway results in uniform Cr isotope fractionation at different electron donor concentrations  
434 (*i.e.*, Sikora et al., 2008; Basu et al., 2014; Zhang et al., 2019). Further, the extracellular

435 reduction pathway for Se(IV) is not impacted by mass transfer limitation of Se(IV) to the  
436 bacterial cell and this explains the relatively good agreement for isotope fractionation  
437 between sediment slurry experiments for particle-bound natural microbial consortia ( $\epsilon = -$   
438 8.4‰; Ellis et al., 2003) and our pure culture study with free-living cells ( $\epsilon = -6.2$  to  $-7.8\%$ ).

## 439 **5. Implications**

440 Given the distinctive amounts of Se isotope fractionation for microbial reduction of the two  
441 Se-oxyanions, Se isotope ratios can, in principle, shed light on the processing of Se-  
442 oxyanions in both modern and ancient environments.

### 443 *5.1. Modern environments.*

444 Selenium stable isotope ratios have been previously used as indicators for Se sources and  
445 cycling in aquifers, lakes, soils and sediments (Clark and Johnson 2010; Schilling et al.,  
446 2015; Basu et al., 2016). Microbial reduction of Se reduces the mobility of Se from soluble  
447 poorly adsorbed Se(VI), to soluble strongly adsorbed Se(IV), to solid Se(0).

448 Our  $\epsilon$  values can be understood as reference values to estimate the extent of Se  
449 reduction for bacterial groups most commonly found in the environment. A clear indicator of  
450 the reduction of Se(VI) to Se(IV) is the enrichment of  $^{82}\text{Se}$  in Se(VI) or Se(IV) in  
451 groundwater or porewater while the reduced Se species in sediments and soils is enriched in  
452  $^{76}\text{Se}$ . If microbial Se reduction is the dominant reaction mechanism in nature, this should be  
453 reflected by shifts in  $\delta^{82/76}\text{Se}$  ratios according to the aqueous speciation of Se and the  $\epsilon$  for  
454 that particular reaction.

455 In groundwater systems, we can infer the  $\epsilon$  for Se removal mechanism from  $\delta^{82/76}\text{Se}$  of  
456 Se(VI) and Se(IV) measured in the same sample (Schilling et al., 2015; Basu et al., 2016).  
457 The Microbial reduction of Se-oxyanions in a groundwater plume moving through a redox  
458 gradient will fractionate  $\delta^{82/76}\text{Se}$  of both the reactant and the product. This fractionation

459 combined with the reactive transport of Se should lead to a systematic pattern of  $\delta^{82/76}\text{Se}$   
460 induced by a distillation effect in the groundwater. With progressive reduction along the flow  
461 path, Se-oxyanions will become isotopically heavy. For instance, Basu et al. (2016) observed  
462 increasing  $\delta^{82/76}\text{Se}$  with decreasing Se(VI) concentrations in an aquifer along the redox  
463 gradient at an *in-situ* recovery mining site. However, along the flow path of groundwater the  
464 rate of microbial Se reduction may vary depending on the organic carbon content of the  
465 aquifer, and the bacterial population density. This variation in the Se reduction rates can  
466 systematically affect the  $\epsilon$ , which is determined by the difference in  $\delta^{82/76}\text{Se}$  between Se(VI)  
467 and Se(IV) of the same sample.

468 The dependence of  $\epsilon$  on the Se(VI) reduction rate has important implications for predicting  
469 Se removal/accumulation patterns in modern settings based on Se isotope ratios. Our  
470 experimental results suggest a higher  $\epsilon$  at low Se(VI) reduction rates generally found in  
471 terrestrial sediments with low organic carbon. In contrast, lower  $\epsilon$  is expected in geochemical  
472 settings with high Se(VI) reduction rate commonly found after organic carbon amendment  
473 (*i.e.*, acetate) at active bioremediation sites. Our results suggest that the  $\epsilon$  inferred from water  
474 samples may be used to estimate the Se(VI) reduction rate, which is difficult to determine  
475 accurately in open systems. Similarly, if the Se(VI) reduction rate is known, an appropriate  
476  $\epsilon$  can be determined for calculating the extent of remediation for active remediation sites  
477 using rate- $\epsilon$  relationship. Therefore, any quantitative interpretation of the groundwater Se  
478 isotope ratios is predicated on the knowledge of the size of the intrinsic  $\epsilon$  and the factors that  
479 control  $\epsilon$  at a geochemical setting.

480 Sedimentary Se isotope ratios may provide a complimentary view of the relationship  
481 between reduction rate of Se oxyanions and  $\epsilon$ . The  $\delta^{82/76}\text{Se}$  values of different Se soil pools in  
482 agricultural seleniferous soils vary up to 13‰ (Schilling et al., 2015). The isotopically heavy

483 adsorbed Se(IV) in the agricultural seleniferous soils suggest Se isotope fractionation by  
484 microbial reduction of Se(VI) in irrigation water prior to scavenging of the reaction product  
485 Se(IV) by reactive minerals in the soil. Therefore, our laboratory-derived  $\epsilon$  values for  
486 microbial reduction are essential to quantitative determination of the extent of microbial  
487 reduction in the field. Nevertheless, site-specific  $\epsilon$  values should still be obtained from  
488 experiments using the resident Se-reducing microbial community

489

## 490 5.2. Ancient environments

491 The Se isotope signature preserved in rocks and sediments can be used to constrain the  
492 evolution of the biosphere and redox conditions in near surface environments through time  
493 (Wen and Carignan, 2011; Mitchell et al., 2012, 2016; Wen et al., 2014; Stüeken et al.,  
494 2015a, b; Kipp et al., 2017). However, interpreting Se isotope signature preserved in rocks  
495 and sediments is still difficult as (1) bulk rock Se isotope data mask the variability in Se  
496 isotope ratio of various Se phases (*i.e.*, organically-bound, pyritic, adsorbed) in the rocks and  
497 (2) the effects of local versus global controls on Se cycling due to the short oceanic residence  
498 time ( $10^3$  years) of Se species and their low concentrations ( $<1\text{nM}$ ). Therefore, the  
499 application of Se isotopes as a paleoredox proxy relies on experimentally determined  $\epsilon$  values  
500 for microbial reduction of Se-oxyanions. High-resolution isotope analyses with an analytical  
501 precision of 0.2‰ allows to resolve different reaction pathways and fingerprint Se sources  
502 preserved within the rock record.

503 Selenium isotope signature in bulk shales range between -1.5 and +2.2‰ over geological  
504 time (Wen and Carignan, 2011; Mitchell et al., 2012; Pogge von Strandmann et al., 2014;  
505 Stüeken et al., 2015a, b; Mitchell et al., 2016). The sequestration of isotopically light Se has  
506 been reported for shale deposits (Wen and Carignan, 2011; Mitchell et al., 2012; Pogge von  
507 Strandmann et al., 2014; Stüeken et al., 2015a, b) suggesting the partial reduction of Se-

508 oxyanions in suboxic basins. Our results suggest a lower  $\epsilon$  during very rapid removal of  
509 Se(VI), the dominant Se species in the ocean (Conde and Alaejos, 1997), during anoxia  
510 which is consistent with small changes in  $\delta^{82/76}\text{Se}$  in the black shales. However, it is  
511 necessary to extract phase-specific Se (*i.e.*, adsorbed, organic, pyritic) from rocks and  
512 sediments and determine their Se isotope compositions to disentangle microbial reduction of  
513 Se-oxyanions from other reaction pathways (*i.e.*, adsorption and assimilation). It should be  
514 noted that muting of  $\epsilon$  values are expected in semi-closed or open flow through systems  
515 (Shrimpton et al., 2018) like microbial Se reduction in porewater in ancient oceans compared  
516 to  $\epsilon$  values typically observed during Rayleigh distillation in a closed system.

517         In our study, we demonstrate that decreasing microbial activity results in smaller  
518 cSRR, which causes larger Se isotope fractionation and this could ultimately be reflected in  
519 lighter Se isotopic signature in sedimentary Se reservoirs. Despite uncertainties about the Se  
520 concentrations and its speciation in ancient oceans, our results imply a systematic relationship  
521 between the rate of Se reduction and the observed Se isotope fractionation which must be  
522 considered when interpreting  $\delta^{82/76}\text{Se}$  signatures. This relationship can be of great importance  
523 because Se reduction rates may be derived from Se isotope signature preserved in the rock  
524 record. Thus, the Se isotope signatures recorded in ancient sediments should be re-examined  
525 given the influence of Se(VI) reduction rate on the magnitude of Se isotope fractionation.

526 Future studies should be designed to constrain Se isotope fractionation at microbial Se  
527 reduction rates relevant to ancient marine conditions and reconstruct  $\delta^{82/76}\text{Se}$  ratios imprinted  
528 in the rock record. Additionally, phase-specific Se isotope analysis for rocks and sediments,  
529 and quantitative modeling approaches can help to provide further insight into the microbial  
530 Se cycling in the ancient ocean.

## 531 **6. Summary and Conclusions**

532 This study provides the first insights on the variation of Se isotope fractionation for non-  
533 respiring Se reduction by six different bacterial strains (*Geobacter sulfurreducens* PCA,  
534 *Anaeromyxobacter dehalogenans* FRC-W, *Shewanella* sp. (NR), *Enterobacter cloacae*  
535 SLDa1-1, *Desulfitobacterium chlororespirans* Co23 and *Desulfitobacterium* sp. Viet-1). We  
536 demonstrate that under environmentally-relevant experimental conditions (e.g., <42  $\mu\text{M}$  Se;  
537 500  $\mu\text{M}$  electron donor), Se isotope fractionation factors reveal a relatively narrow range for  
538 both Se(VI) and Se(IV) reduction with consistently larger Se isotope fractionation for Se(VI)  
539 ( $\epsilon_{\text{mean}} = -10.6 \pm 1.3\text{‰}$ ) than for Se(IV) reduction ( $\epsilon_{\text{mean}} = -7 \pm 0.6\text{‰}$ ). Based on the present  
540 and previous studies on microbial reduction of Se-oxyanions, we conclude that Se isotopic  
541 fractionation during microbial reduction is controlled by the co-metabolic reaction  
542 pathway(s).

#### 543 **Acknowledgement**

544 The authors wish to thank Linden Schneider for helping with the experiment. This study was  
545 financially supported by the Netherlands Organisation for Scientific Research grant number  
546 820.02.007.

547

548 **References**

- 549 Basu A., Schilling K., Brown S.T., Johnson T.M., Christensen J., Hartmann M., Reimus P.,  
550 Heikoop J., WoldeGabriel G., DePaolo D.J. (2016) Selenium isotope ratios  
551 groundwater redox indicators: Detecting natural attenuation of Se at an In Situ  
552 Recovery U mine *Environ. Sci. Technol.* **50**, 10833-10842.
- 553 Basu A., Johnson T.M., Sanford R.A. (2014) Cr isotope fractionation factors for Cr(VI)  
554 reduction by a metabolically diverse group bacteria. *Geochim. Cosmochim. Acta* **142**,  
555 349-361.
- 556 Basaglia M. Toffanin A., Baldan E. Bottegal M., Shapleigh J.P., Casella S. (2007) Selenite-  
557 reducing capacity of the cooper-containing nitrite reductase of *Rhizobium sllae*.  
558 *FEMS Microbiol. Lett.* **269**, 124-130.
- 559 Bébien M., Kirsch J., Mejean V., Vermeglio A. (2002) Involvement of a putative  
560 molybdenum enzyme in the reduction of selenate by *Escherichia coli*. *Microbiol.* 148:  
561 3865-3872.
- 562 Brock T.D. (1971) Microbial growth rates in nature. *Bacteriol. Rev.* 35: 39-58.
- 563 Carignan J., Wen H. (2007) Scaling NIST SRM3149 for Se isotope analysis and isotopic  
564 variations of natural samples. *Chem. Geol.* **242**, 347-350.
- 565 Clark S.K., Johnson T.M. (2008) Effective isotopic fractionation factors for solute removal  
566 by reactive sediments: A laboratory microcosm and slurry study. *Environ. Sci.*  
567 *Technol.* **42**, 7850-7855.
- 568 Clark S.K., Johnson T.M. (2010) Selenium stable isotope investigation into selenium  
569 biogeochemical cycling in a lacustrine environment. Sweitzer Lake, Colorado. *J.*  
570 *Environ. Qual.* **39**, 2200-2210.
- 571 Conde J.E., San Alaejos M. (1997) Selenium concentration in natural and environmental  
572 waters. *Chem. Rev.* 97: 1979-2003.
- 573 Deverel S.J. and Fujii R. (1988) Processes affecting the distribution of selenium in shallow  
574 groundwater of agricultural areas, western San Joaquin Valley, California. *Water*  
575 *Resour. Res.* **24**, 516-524.
- 576 Dreher G.B., Finkelman R.B. (1992) Selenium mobilization in a surface coal mine, Powder  
577 River Basin, Wyoming, USA. *Environ. Geol. Water Sci.* **19**, 155-167.
- 578 Ellis A.S., Johnson T.M., Bullen T.D., Herbel M.J. (2003) Stable isotope fractionation of  
579 selenium by natural microbial consortia. *Chem. Geol.* **195**, 119-129.
- 580 Fordyce, F.M. 2013. Selenium deficiency and toxicity in the environment. IN: Essentials of  
581 Medical Geology, O. Selinus (eds.) British Geol. Survey. 375-416.
- 582 He Q., Sanford R.A. (2002) Induction characteristics of reductive dehalogenation in the  
583 ortho-halophenol-respiring bacterium, *Anaeromyxobacter dehalogenans*.  
584 *Biodegradation* **13**, 307-316.
- 585 Herbel M.J., Johnson T.M., Oremland R.S., Bullen T.D. (2000) Fractionation of selenium  
586 isotopes during bacterial respiratory reduction of selenium oxyanions. *Geochim.*  
587 *Cosmochim. Acta* **64**, 3701-3709.
- 588 Heumann K.G. (1992) Isotope dilution mass spectrometry. *Int. J. Mass Spectrom.* **118-119**,  
589 575-592.
- 590 Howard H.J. (1977) Geochemistry of selenium: Formation of ferroselite and selenium  
591 behavior in the vicinity of oxidizing sulfide and uranium deposits. *Geochim.*  
592 *Cosmochim. Acta* **41**, 1665-1678.
- 593 Hunter W.J., Manter D.K. (2008) Bio-reduction of selenite to elemental red selenium by  
594 *Tetrathibacter kashmirensis*. *Curr. Microbiol.* **57**, 83-88.
- 595 Hunter W.J., Manter D.K. (2009) Reduction of selenite to elemental red selenium by  
596 *Pseudomonas* sp. strain CA5. *Curr. Microbiol.* **58**, 493-498.



- 597 Kessi J., Hanselmann K.W. (2004) Similarities between the abiotic reduction of selenite with  
598 glutathione and the dissimilatory reaction mediated by *Rhodospirillum rubrum*.  
599 *Appl. Environ. Microbiol.* **65**, 4734-4740.
- 600 Kipp M.A., Stueken E.E., Bekker A., Buick R. (2017) Selenium isotopes record extensive  
601 marine suboxia during the Great Oxidation Event. *Proc. Natl. Acad. Sci.* **114**, 875-  
602 880.
- 603 Kuroda M., Yamashita M., Miwa E., Imao K., Fujimoto N., Ono H., Nagano K., Sei K., Ike  
604 M. (2011). Molecular cloning and characterization of the *srdBCA* operon, encoding  
605 the respiratory selenate reductase complex, from the selenate-reducing bacterium  
606 *Bacillus selenatarsenatis* SF-1. *J. Bacteriol.* **193**, 2141-2148.
- 607 Lemly A.D. (2004) Aquatic selenium pollution is a global environmental safety issue.  
608 Selenium transport and bioaccumulation in aquatic ecosystems: A proposal for water  
609 quality criteria based on hydrological units. *Ecotoxicol. Environ. Safe.* **42**, 150-156.
- 610 Ma, J., Kobayashi, D.Y., Yee, N. 2009. Role of menaquinone biosynthesis genes in selenate  
611 reduction by *Enterobacter cloacae* SLD1a-1 and *Escherichia coli* K12. *Environ.*  
612 *Microbiol.* **11**, 149-158.
- 613 Macy, J.M., Rech, S., Auling, G., Dorsch, M., Stackebrandt, E., Sly, L.I. 1993. *Thauera*  
614 *selenatis* gen. nov., sp. nov., a member of the beta subclass of Proteobacteria with a  
615 novel type of anaerobic respiration. *Int. J. Syst. Bacteriol.* **43**, 135-142.
- 616 Mars J.C. and Crowley J.K. (2003) Mapping mine wastes and analyzing areas affected by  
617 selenium-rich water runoff in southeast Idaho using AVIRIS imagery and digital  
618 elevation data. *Remote Sens. Environ.* **84**, 422-436.
- 619 Martin A.J., Simposon S., Fawcett S., Wiramanaden C.  
620 I.E., Pickering I.J., Belzile N., Chen Y.W., London J., Wallschaeger D. (2011).  
621 Biogeochemical mechanisms of selenium exchange between water and sediments in  
622 two contrasting lentic environments. *Environ. Sci. Technol.* **45**, 2605-2612.
- 623 Mitchell, K., Mason, P.R.D., van Cappellen, P., Johnson, T.M., Gill, B.C., Owens, J.D., Diaz,  
624 J., Ingall, E.D., Reichart, G.J., Lyons, T.W. 2012. Selenium as paleo-oceanographic  
625 proxy: A first assessment. *Geochim. Cosmochim. Acta* **89**, 302-317.
- 626 Meseck S. and Cutter G (2012) Selenium behavior in San Francisco Bay sediments  
627 *Estuaries Coast* **35**: 646-657.
- 628 Mitchell, K., Mansoor S.Z., Mason, P.R.D., Johnson, T.M., van Cappellen, P. (2016)  
629 Geological evolution of the marine selenium cycle: Insights from the bulk shale  
630  $\delta^{82/76}\text{Se}$  record and isotope mass balance modeling. *Earth Planet Sci. Lett.* **441**, 178-  
631 187.
- 632 Muscatello J.R., Belknap A.M. and Janz D.M. (2008) Accumulation of selenium in aquatic  
633 systems downstream of uranium mining operation in northern Saskatchewan, Canada.  
634 *Environ. Poll.* **156**, 387-393.
- 635 Nancharaiyah Y.V., Lens P.N.L (2015) Ecology and biotechnology of selenium-respiring  
636 bacteria. *Microbiol. Mol. Biol. Rev.* **79**, 61-80.
- 637 Oremland R.S., Hollibaugh J.T., Maest A.S., Presser T.S., Miller L., Culbertson C. (1989)  
638 Selenate reduction to elemental selenium by anaerobic bacteria in sediments and  
639 culture: Biogeochemical significance of a novel, sulfate-independent respiration.  
640 *Appl. Environ. Microbiol.* **55**, 2333-2343.
- 641 Parida K.M., Gorai B., Das N.N. and Rao S.B. (1997) Studies on ferric oxide hydroxides: III.  
642 Adsorption of selenite ( $\text{SeO}_3^{2-}$ ) on different forms of iron oxyhydroxides. *J. Coll.*  
643 *Interf. Sci.* **185**, 355-362.
- 644 Peak D. (2006) Adsorption mechanisms of selenium oxyanions at the aluminum oxide/water  
645 interface. *J. Coll. Interf. Sci.* **303**, 337-345.

- 646 Peak, D. and Sparks D.L. (2002) Mechanisms of selenate adsorption on iron oxides and  
647 hydroxides. *Environ. Sci. Technol.* **36**, 1460-1466.
- 648 Pearce C.I., Patrick R.A.D., Law N., Charnock J.M., Coker V.S., Fellows J.W., Oremland  
649 R.S., and Lloyd J.R. (2009) Investigating different mechanisms for biogenic selenite  
650 transformations: *Geobacter sulfurreducens*, *Shewanella oneidensis* and *Veillonella*  
651 *atypical*. *Environ. Technol.* **30**, 1313-1326.
- 652 Pogge von Strandmann P.A.E., Stüeken E.E., Elliot T., Poulton S.W. Dehler C.M., Canfield  
653 D.E., Catling D.C. (2015) Selenium isotope evidence for progressive oxidation of the  
654 Neoproterozoic biosphere. *Nature Commun.* **6**.
- 655 Presser T.S. and Ohlendorf H.M. (1987) Biogeochemical cycling of selenium in San Joaquin  
656 Valley, California, USA. *Environ. Managem.* **11**, 805-821.
- 657 Ridley H., Watts C.A., Richardson D.J. and Butler C.S. (2006) Resolution of distinct  
658 membrane-bound enzymes from *Enterobacter cloacae* SLD1a-1 that are responsible  
659 for selective reduction of nitrate and selenate oxyanions. *Appl. Environ. Microbiol.*  
660 **72**, 5173 - 5180.
- 661 Sabaty M., Avazeri C., Pignol D., Vermeglio A. (2001) Characterization of the reduction of  
662 selenate and tellurite by nitrate reductases. *Appl. Environ. Microbiol.* **67**, 5122-5126.
- 663 Schilling K., Johnson T.M. and Mason P.R.D. (2014) A sequential extraction technique for  
664 mass-balanced stable selenium isotope analysis of soil samples. *Chem. Geol.* **381**,  
665 125-130.
- 666 Schilling, K., Johnson T.M., Dhillon K.S. and Mason P.R.D. (2015) Fate of selenium in soils  
667 at a seleniferous site recorded by high precision Se isotopes measurements. *Environ.*  
668 *Sci. Technol.* **49**, 9690-9698.
- 669 Shrimpton H.K., Jamieson-Hanes J.H., Ptacek C.J., Blowes D.W. (2018) Real-time XANES  
670 measurement of Se reduction by zerovalent iron in a flow-through cell, and  
671 accompanying Se isotope measurements. *Environ. Sci. Technol.* **52**, 9304-9310.
- 672 Schröder I., Rech S., Krafft T. and Macy J.M. (1997) Purification and characterization of the  
673 selenate reductase from *Thauera selenatis*. *J. Biol. Chem.* **272**, 23765-23768.
- 674 Scott K., Lu X., Cavanaugh C. and Liu J. (2004) Optimal methods for estimating kinetic  
675 isotope effects from different forms of the Rayleigh distillation equation. *Geochim.*  
676 *Cosmochim. Acta* **68**, 433-442.
- 677 Sikora E.R., Johnson T.M. and Bullen T.D. (2008) Microbial mass-dependent fractionation  
678 of chromium isotopes. *Geochim. Cosmochim. Acta.* **72**, 3631-3641.
- 679 Stillings L.L. and Amacher M.C. (2010). Kinetics of selenium release in mine waste from the  
680 Meade Peak Phosphatic Shale, Phosphoria Formation, Wooley Valley, Idaho, USA.  
681 *Chem. Geol.* **269**, 113-123.
- 682 Stolz J.F. and Oremland R.S. (1999) Bacterial respiration of arsenic and selenium. *FEMS*  
683 *Microbiol. Rev.* **23**, 615-627.
- 684 Stolz J.E., Basu P., Santini J.M. and Oremland R.S. (2006) Arsenic and selenium in microbial  
685 metabolism. *Annu. Rev. Microbiol.* **60**, 107-130.
- 686 Stüeken E.E., Buick R., Bekker A., Catling D., Foriel J., Guy B.M., Kah L.C., Machel H.G.,  
687 Montanez I.P., Poulton S.W. (2015a). The evolution of the global selenium cycle:  
688 Secular trends in Se isotopes and abundances. *Geochim Cosmochim. Acta* **162**, 109-  
689 125.
- 690 Stüeken E.E., Buick R., Anbar A.D. (2015b) Selenium isotopes support free O<sub>2</sub> in the latest  
691 Archean. *Geology* **43**, 259-262.

- 692 Switzer-Blum J.S., Bindi A.B., Buzzelli J., Stolz J.F. Oremland, R.S. (1998) *Bacillus*  
693 *arsenicosenenatis*, sp. Nov., and *Bacillus selenitireducens*, sp. Nov.: two  
694 haloalkaliphiles from MonoLake, California that respire oxyanions of selenium and  
695 arsenic. *Arch. Microbiol.* **171**, 19-30.
- 696 Theissen J. and Yee, N. (2014) The molecular basis for selenate reduction in *Citrobacter*  
697 *freundii*. *Geomicrobiol. J.* **31**, 875 - 883.
- 698 Watts C.A., Ridley H., Condie K.L., Leaver J.T., Richardson D.J. and Butler C.S. (2003)  
699 Se(VI) reduction by *Enterobacter cloacae* SLD1a-1 is catalysed by a molybdenum-  
700 dependent membrane-bound enzyme that is distinct from the membrane-bound nitrate  
701 reductase. *FEMS Microbiol. Lett.* **228**, 273-279.
- 702 Wen H.J. and Carignan J. (2011) Selenium isotope trace the source and redox processes in  
703 the black shale-hosted Se-rich deposit in China. *Geochim. Cosmochim. Acta* **75**, 1411-  
704 1427.
- 705 Wen H.J., Carignan J., Chu X., Fan, H.F., Cloquet C., Huang J., Zhang, Y. and Chang, H.  
706 (2014) Selenium isotopes trace anoxic and ferruginous seawater conditions in the  
707 Early Cambrian, *Chem. Geol.* **390**, 164-172.
- 708 Yee N. and Kobayashi, D.Y. (2008) Molecular genetics of selenate reduction by  
709 *Enterobacter cloacae* SLD1a-1. *Advan. Appl. Microbiol.* **64**, 107-123.
- 710 Zhang Q., Amor K., Galer S.J.G., Thompson I., Porcelli D. (2019) Using stable isotope  
711 fractionation factors to identify Cr(VI) reduction pathways: Metal-minerals-microbe  
712 interaction. *Water Res.* **151**, 98-109.
- 713 Zhu J.M., Johnson T.M., Clark S.K. and Zhu X.K. (2008) High precision measurements of  
714 selenium isotopic composition by hydride generation multiple collector inductively  
715 coupled plasma mass spectrometry with a <sup>74</sup>Se- <sup>77</sup>Se double spike. *Chin. J. Anal.*  
716 *Chem.* **36**, 1385-1390.
- 717 Zhu J.M., Johnson T.M., Clark S.K., Zhu X.K., Wang X. (2014) Selenium redox cycling  
718 during weathering of Se-rich shales: A selenium isotope study. *Geochim. Cosmochim.*  
719 *Acta* **126**, 228-249.
- 720

721

## Figure Caption

722 **Figure 1.** Phylogenetic tree showing currently described Se(VI) and Se(IV)-reducing bacteria  
723 Species names are shown in italics. Red marked species represent the bacterial strains studied  
724 in this work. Also indicated the taxonomic classes of bacteria.

725

726 **Figure 2.** Time series (batch experiments) of Se(VI) reduction at 30°C with 500 μM of  
727 acetate (*Enterobacter cloacae SLD1a-1*) or lactate (*Desulfitobacterium chlororespirans*  
728 *Co23*, *Desulfitobacterium sp. Viet-1*) as electron donor. Heat kill control with cells from  
729 *Desulfitobacterium chlororespirans Co23* incubated at 30°C with 500 μM of acetate. The  
730 analytical uncertainty Se concentration is less than 1% and close to the size of the symbols.

731

732 **Figure 3.** Values of  $\delta^{82/76}\text{Se}$  of Se(VI) versus remaining Se(VI) during microbial reduction in  
733 closed system (batch experiments) Modelled lines (dashed) follow a predicted Rayleigh  
734 fractionation process. Uncertainties ( $\pm 2$  SD) are close to the size of the symbols. For the heat-  
735 kill control the error bars show the root mean square error (RMS) of replicate measurements  
736 as described in section 2.5.

737

738 **Figure 4.** Normalized cell-specific reduction rate (cSRR) and Se isotopic fractionation ( $\epsilon$ ) by  
739 phylogenetically diverse bacteria **(A)** reduction of Se(VI) and **(B)** reduction of Se(IV). The  
740 error bars correspond to standard deviation ( $\pm 2$  SD) of  $\epsilon$ 's from duplicate batch experiments  
741 (x-axis), and error (%) of cSRR calculated from repeated cell-counting measurements (y-  
742 axis). For some data points, the error bars are within the size of the symbol.

743

744 **Figure 5.** TEM images of *Enterobacter cloacae SLD1a-1* grown at 30°C under anoxic  
745 conditions in presence of acetate as electron donor and **(A)** Se(VI) or **(B)** Se(IV). Red arrows  
746 indicate the presence of intracellular (A) or extracellular (B) Se(0) as reduction product.  
747 Scale bars represent 0.2 μM.

748

749 **Figure 6.** Time series (batch experiment) of Se(VI) reduction at 30°C with 500 μM of lactate  
750 (*Desulfitobacterium chlororespirans Co23*, *Desulfitobacterium sp. Viet-1*, *Shewanella sp.*  
751 (NR)) or acetate (*Enterobacter cloacae SLD1a-1*, *Anaeromyxobacter FRC-W*, *Geobacter*  
752 *sulfurreducens PCA*.) as electron donor. The analytical uncertainty Se concentration is less  
753 than 1% and close to the size of the symbols.

754 **Figure 7.** Values of  $\delta^{82/76}\text{Se}$  of Se(IV) versus remaining Se(IV) during microbial reduction in  
755 closed system (batch experiments). Modelled lines (dashed) show predicted Rayleigh  
756 fractionation. Uncertainties ( $\pm 2$  SD) are close to the size of the symbols.

Table 1. List of bacterial strains investigated in this study

<b>Bacterial strain</b>	<b>Gram strain</b>	<b>Electron acceptor</b>	<b>Electron donor</b>
<i>Enterobacter cloacae</i> SLD1a-1	-	Se(VI)/Se(IV)	Acetate
<i>Desulfitobacterium chlororespirans</i> Co23	+	Se(VI)/Se(IV)	Lactate
<i>Desulfitobacterium sp.</i> Viet-1	+	Se(VI)/Se(IV)	Lactate
<i>Geobacter sulfurreducens</i> PCA	-	Se(IV)	Acetate
<i>Anaeromyxobacter dehalogenans</i> FRC-W	-	Se(IV)	Acetate
<i>Shewanella sp.</i> (NR)	-	Se(IV)	Lactate

Table 2. Reduction rate [ $t_{50\%}$  in days] and cell-specific reduction rate (cSRR) of investigated bacterial strains

Bacterial strain	Electron acceptor	Initial Se ( $\mu\text{M}$ )	Time for 50% reduction ( $t_{50\%}$ ) (d)	Normalized cSRR ( $10^{-17}$ mol cell $^{-1}$ d $^{-1}$ )
<i>Enterobacter cloacae</i> SLD1a-1	Se(VI)	30	1.13	0.24
	Se(IV)	9	1.03	5.68
<i>Desulfitobacterium chlororespirans</i> Co23	Se(VI)	42	41.25	0.11
		9	2.31	0.29
			1.27	0.45
	Se(IV)	9	0.42	0.51
			0.71	0.31
<i>Desulfitobacterium sp.</i> Viet-1	Se(VI)	47	1.10	0.34
			0.79	1.22
		13	3.80	0.98
			3.85	1.30
	Se(IV)	9	3.10	0.65
			2.49	0.85
<i>Geobacter sulfurreducens</i> PCA	Se(IV)	13	3.10	0.28
		8	0.49	0.92
			0.66	1.14
		15	0.63	0.81
			0.55	1.32
<i>Anaeromyxobacter dehalogenans</i> FRC-W	Se(IV)	13	0.51	0.78
<i>Shewanella sp.</i> (NR)	Se(IV)	19	2.37	0.53
		13	1.60	2.17

Table 3. Magnitude of isotopic fractionation  $\epsilon$  of Se(VI) and Se(IV) reduction by various bacterial strains

Bacterial strain	Electron acceptor	Initial Se concentration ( $\mu\text{M}$ )	Electron donor concentration ( $\mu\text{M}$ )	$\epsilon$ (‰) $^{82/76}\text{Se}$ $\pm 2\text{s.e.}$	Number of experiments
<i>Enterobacter cloacae</i> SLD1a-1	Se(VI)	30	500	-11.5 $\pm$ 0.5	2
	Se(IV)	9	500	-7.6 $\pm$ 0.3	1
<i>Desulfitobacterium chlororespirans</i> Co23	Se(VI)	42	500	-11.8 $\pm$ 0.6	1
		9	500	-11.3 $\pm$ 0.2	2
	Se(IV)	9	500	-7.8 $\pm$ 0.8	2
<i>Desulfitobacterium sp.</i> Viet-1	Se(VI)	47	500	-9.3 $\pm$ 0.5	2
		13	500	-9.2 $\pm$ 0.2	2
	Se(IV)	9	500	-7.3 $\pm$ 0.2	2
<i>Geobacter sulfurreducens</i> PCA	Se(IV)	13	500	-6.3 $\pm$ 0.6	2
		8	2000	-7.0 $\pm$ 0.4	3
		15	10000	-7.3 $\pm$ 0.5	3
<i>Anaeromyxobacter dehalogenans</i> FRC-W	Se(IV)	13	500	-6.3 $\pm$ 0.5	1
<i>Shewanella sp.</i> (NR)	Se(IV)	19	500	-6.9 $\pm$ 0.2	1
		13	500	-6.2 $\pm$ 0.4	1



Figure 1

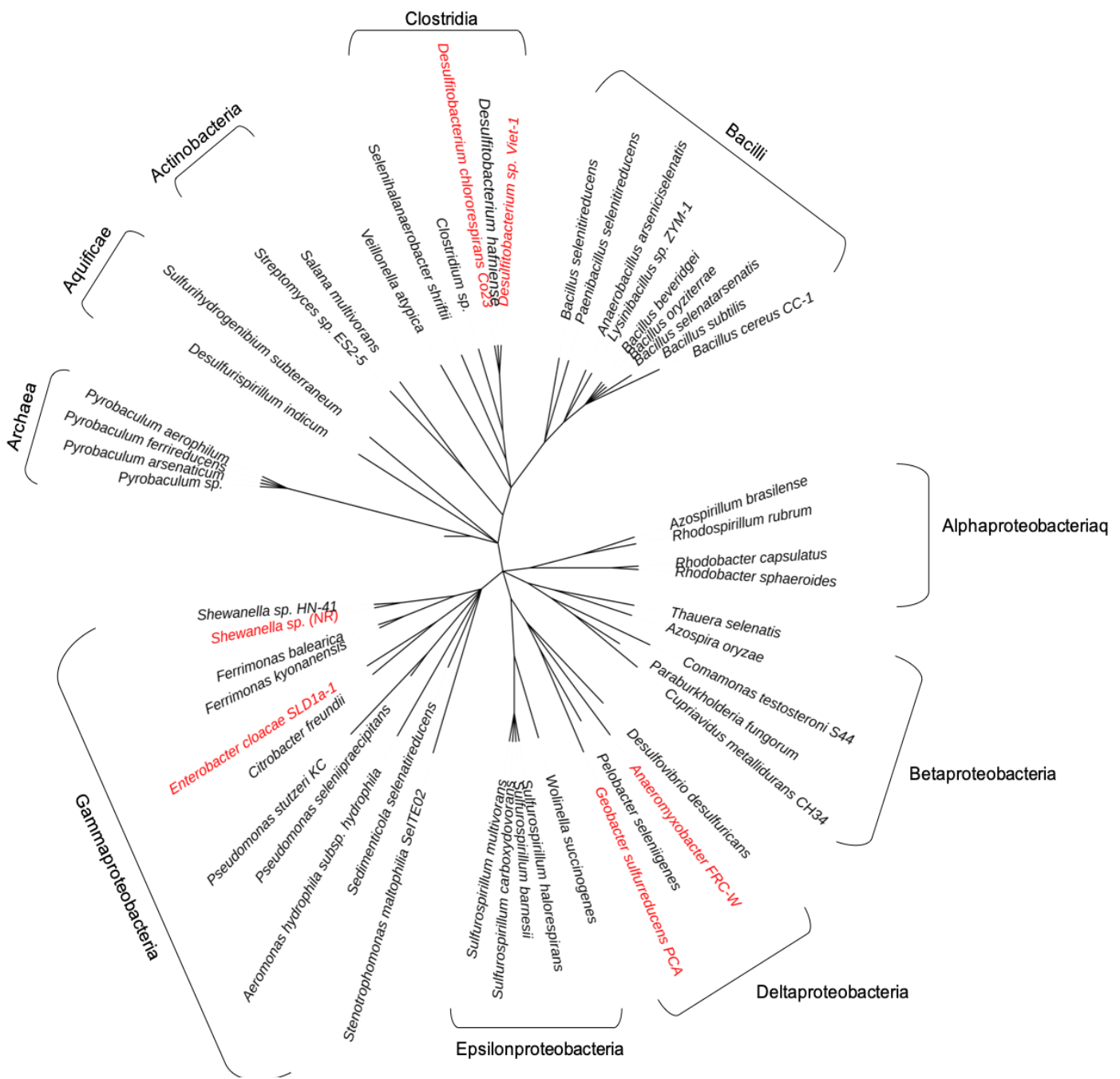


Figure 2

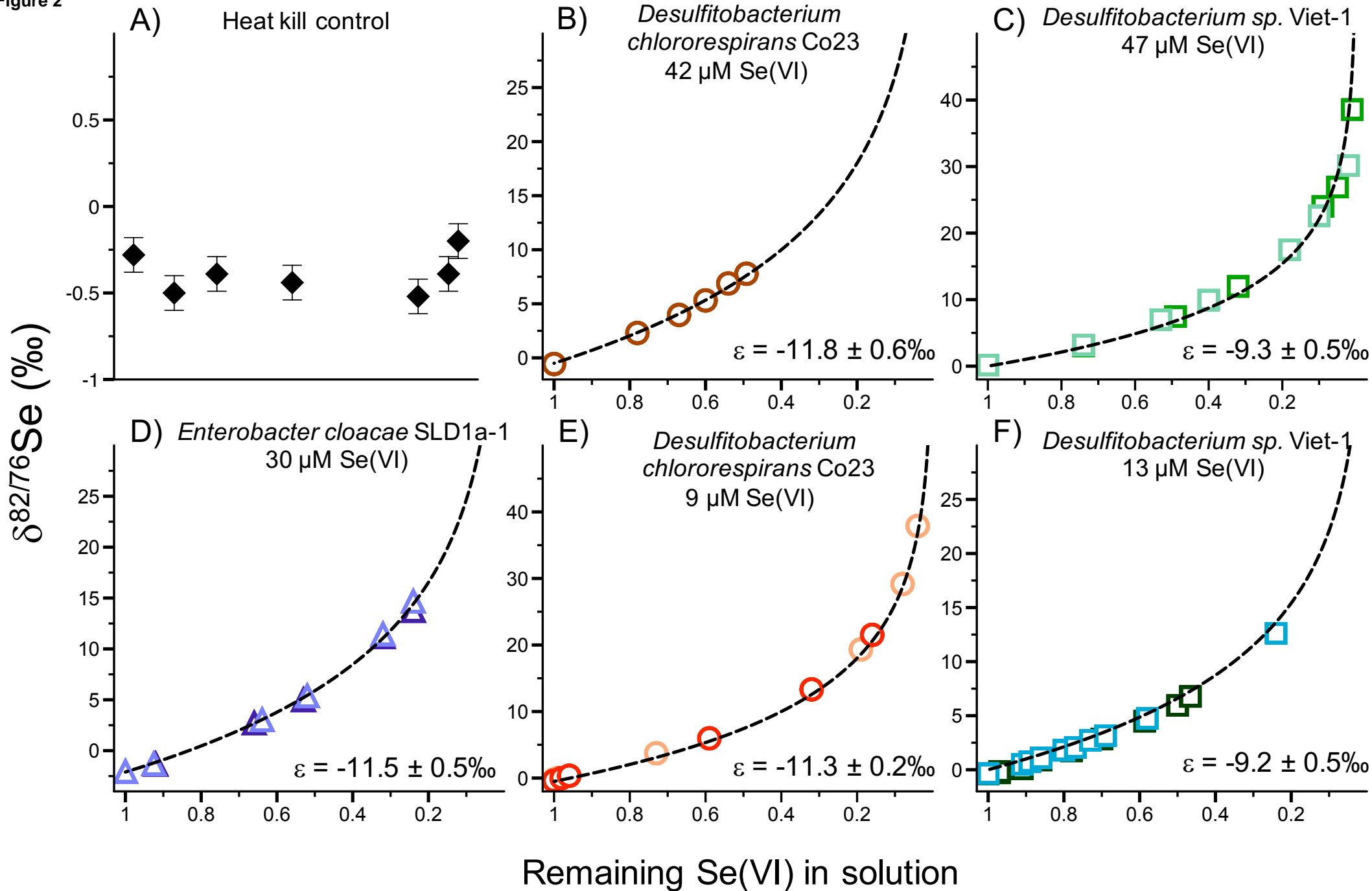


Figure 3

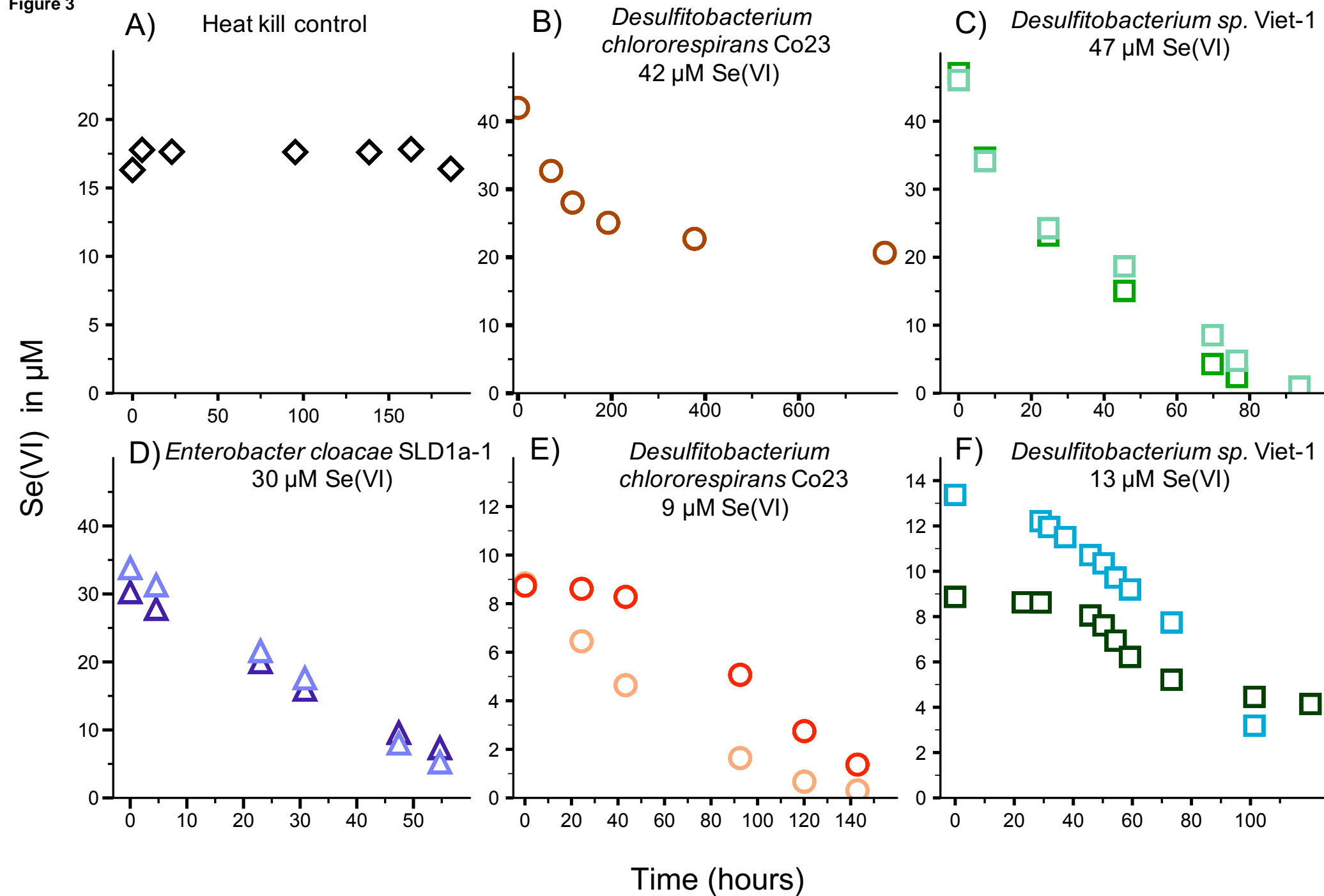
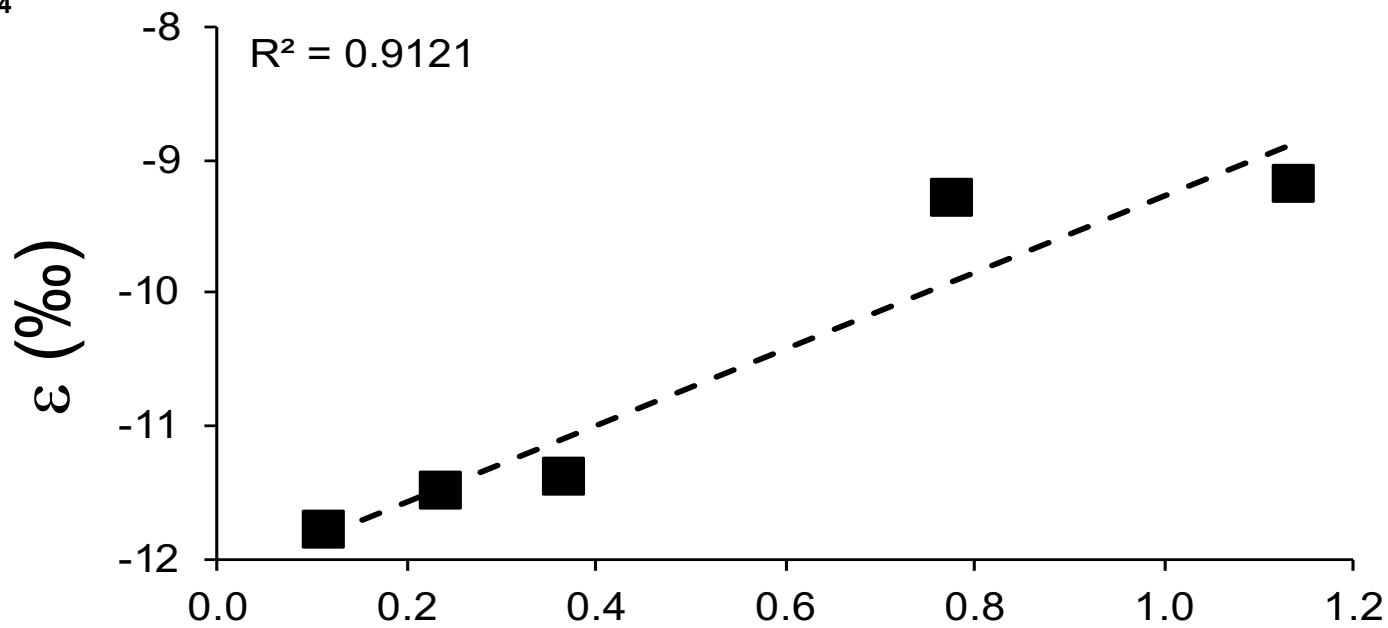


Figure 4

A)



B)

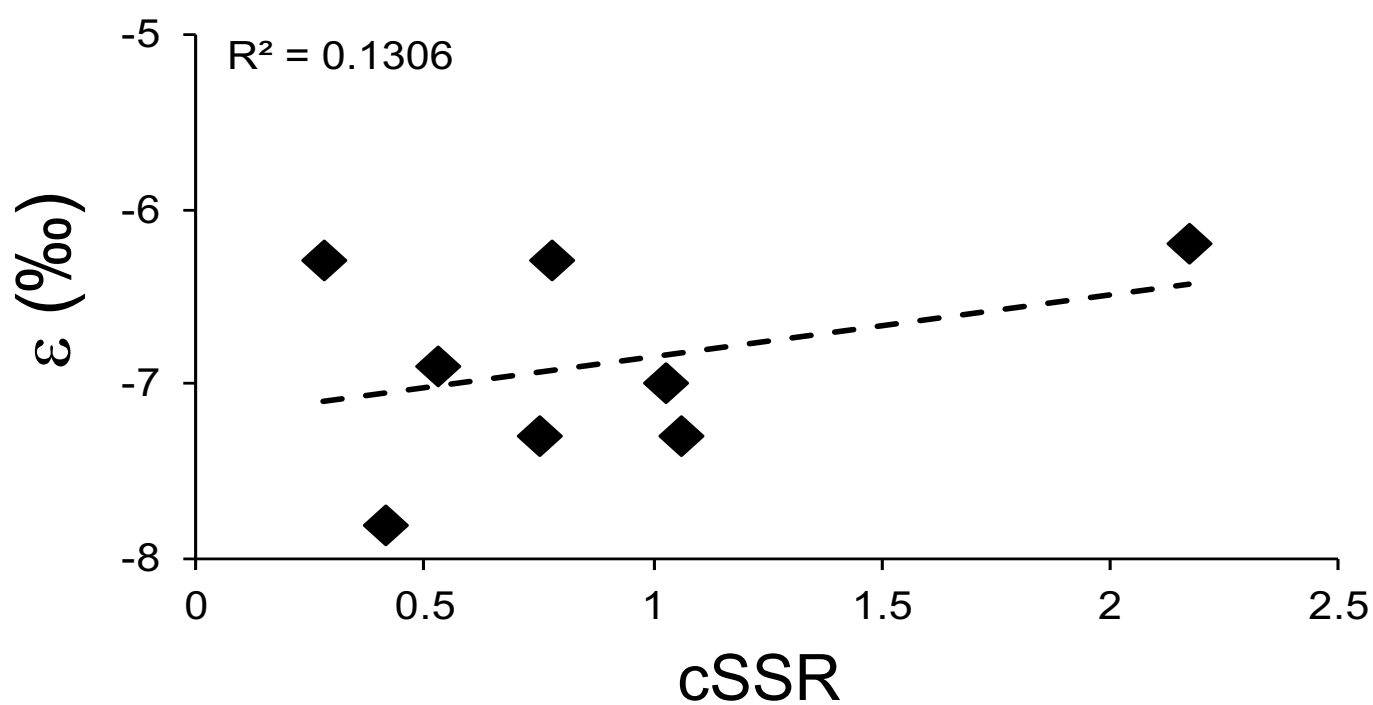


Figure 5

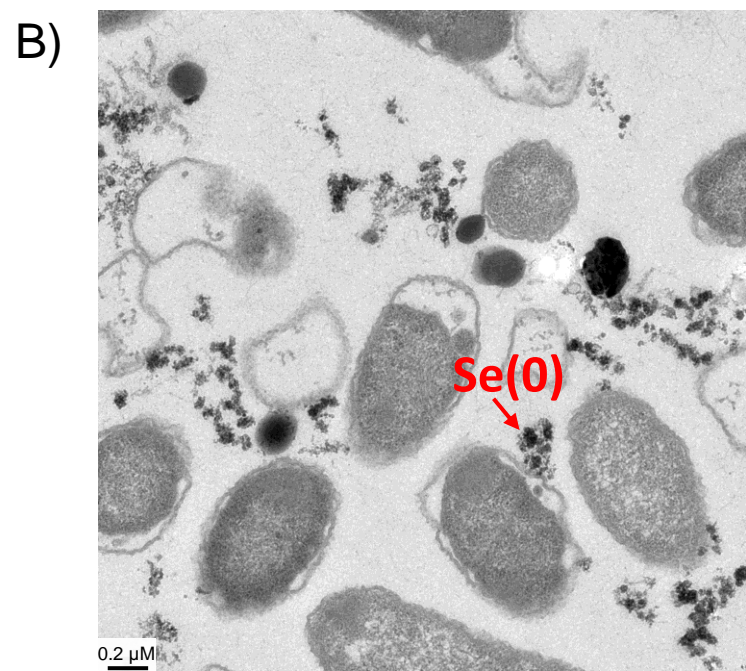
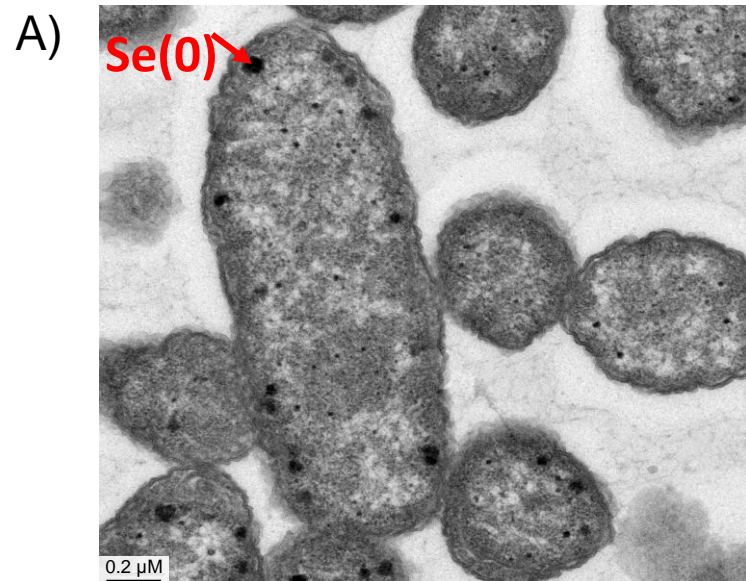


Figure 6

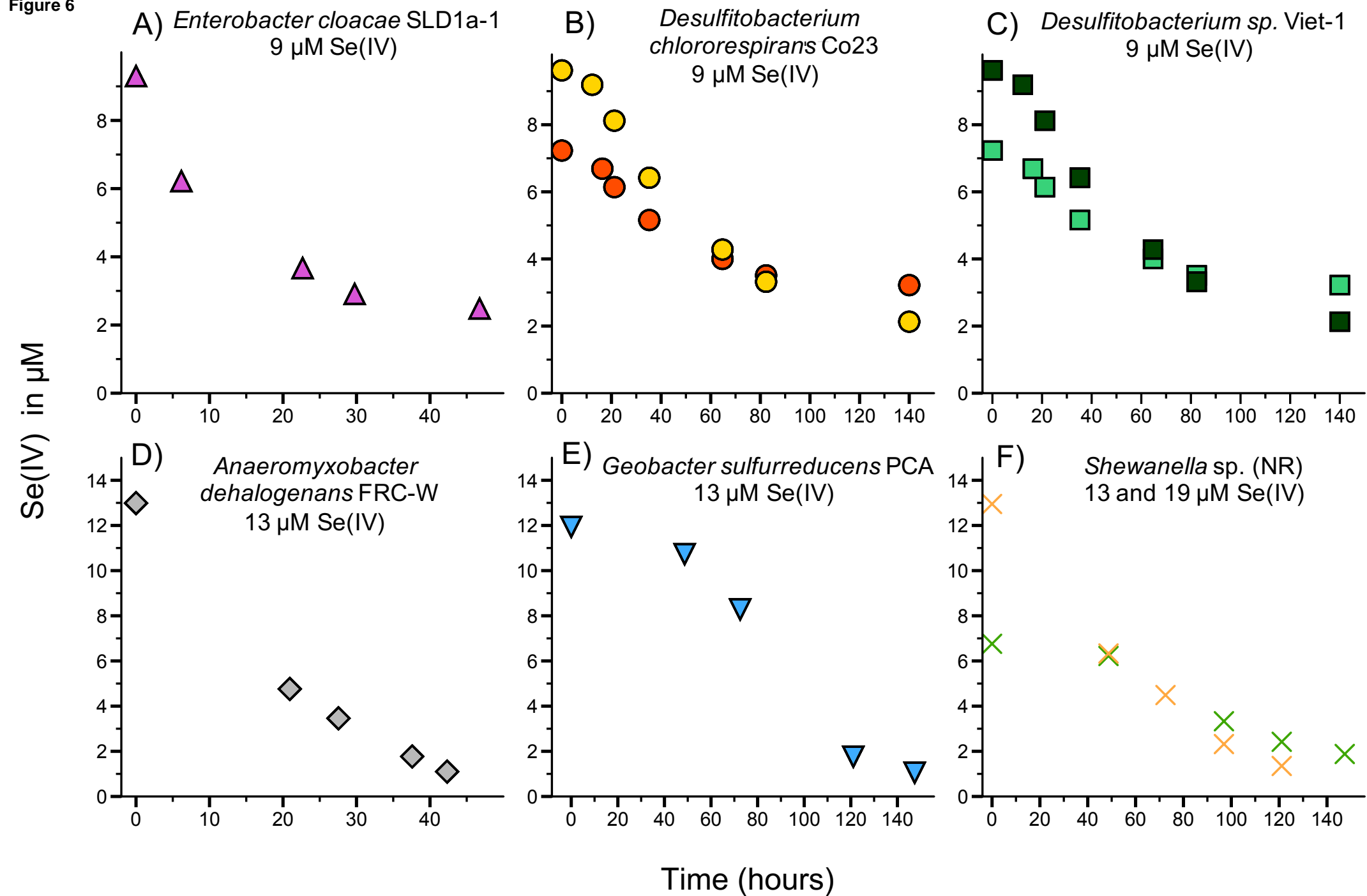
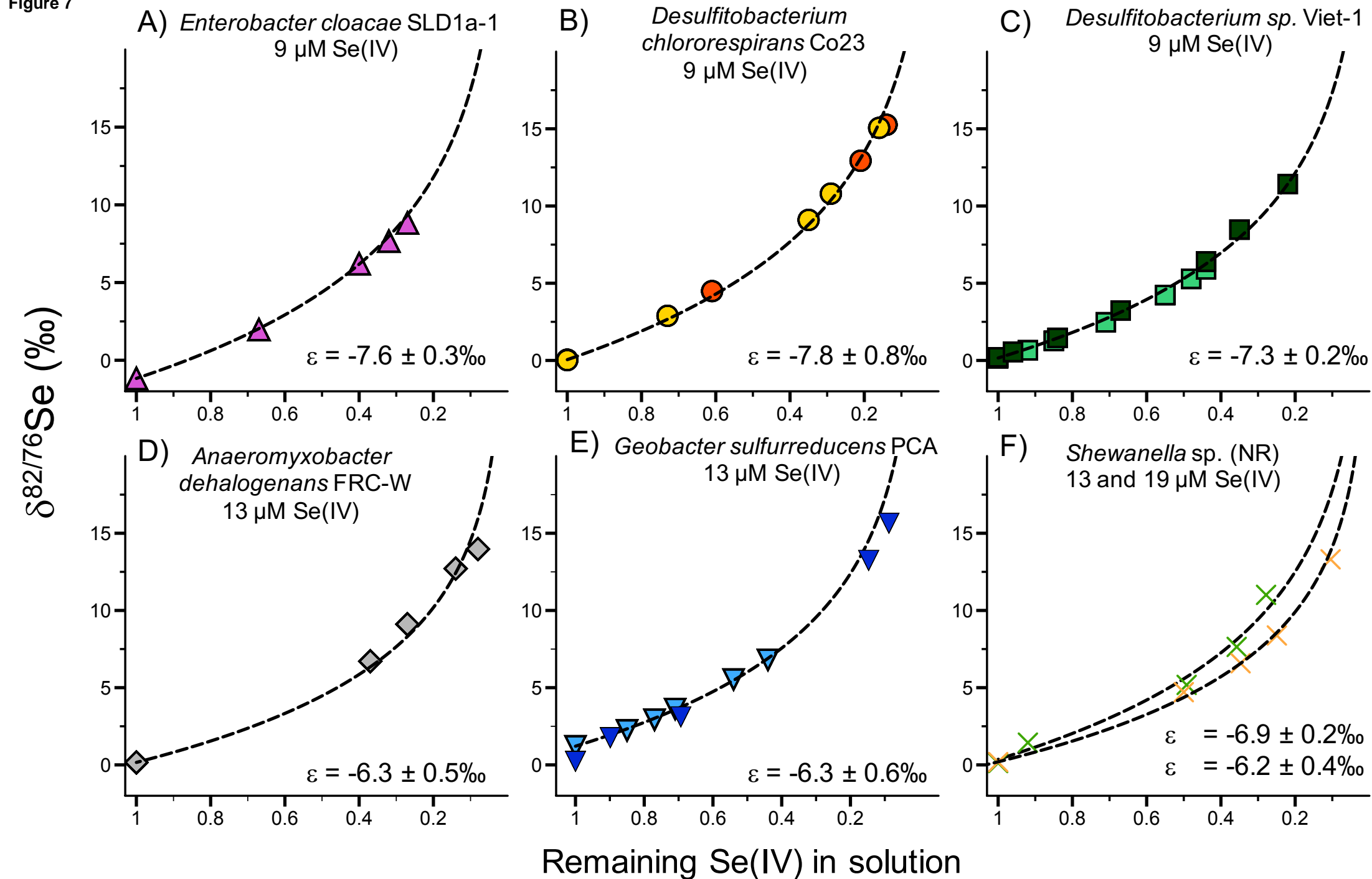


Figure 7



**Electronic Annex**

[Click here to download Electronic Annex: Electronic Annex\\_GCA.docx](#)



**Appendix**

[Click here to download Appendix: APPENDIX\\_GCA.docx](#)